J. Fluid Mech. (1981), *vol.* 102, *pp.* 301–313
Printed in Great Britain

The structure of organized vortices in a free shear layer

By R. T. PIERREHUMBERT† AND S. E. WIDNALL
Department of Aeronautics and Astronautics, Massachusetts Institute of Technology, Cambridge, Massachusetts 02139

(Received 16 July 1979 and in revised form 28 March 1980)

A new family of solutions to the steady Euler equations corresponding to spatially periodic states of a free shear layer is reported. This family bifurcates from a parallel shear layer of finite thickness and uniform vorticity, and extends continuously to a shear layer consisting of a row of concentrated pointlike vortices. The energetic properties of the family are considered, and it is concluded that a vortex in a row of uniform vortices produced by periodic roll-up of a vortex sheet must have a major axis of length approximately 50% or more of the distance between vortex centres; it is also concluded that vortex amalgamation events tend to reduce vortex size relative to spacing. The geometric and energetic properties of the solutions confirm the mathematical basis of the tearing mechanism of shear-layer growth first proposed in an approximate theory of Moore & Saffman (1975).

1. Introduction

Recent experimental evidence indicates that the planar free shear layer has an organized two-dimensional structure over a wide range of Reynolds numbers, and that this structure plays an important role in the growth of the shear layer (Brown & Roshko 1974; Browand & Weidman 1976; Roshko 1976; Winant & Browand 1974). As Saffman & Baker (1979) note in their review article, this has revived considerable interest in solutions to the two-dimensional Euler equations and their properties. In particular, it has been hoped that some features of the coherent two-dimensional shear-layer votices could be explained on the basis of the properties of steady solutions to the two-dimensional Euler equations. It is natural to inquire to what extent the observed vortices not undergoing pairing can be represented as steady states of the Euler equations. Moreover, there is theoretical evidence that in situations where no steady state exists, a vortex will rapidly break up (Moore & Saffman 1971, 1975). Thus, the properties of the stationary solutions may be expected to provide bounds on gross characteristics of even very unsteady vortices. In this paper, we shall present a new family of steady shear-layer vortices and discuss the mechanisms of shear-layer growth in light of their properties. We shall pay particular attention to the energetics of roll-up, pairing and tearing.

Moore & Saffman (1975) calculated the steady state shape of an infinite row of co-rotating vortices under the assumption that each vortex was characterized by constant vorticity within some closed curve embedded in irrotational fluid, and that the net influence of all the neighbours of a given vortex could be approximated by a

† Present address: Department of Meteorology, Massachusetts Institute of Technology.

0022-1120/81/4587-2580 $02.00

uniform plane strain. Although the latter approximation is strictly valid only for vortex cores which are small compared to the space between vortices, the results are apt to be qualitatively correct. Under the assumption of uniform strain, the vortex boundaries are ellipses with semi-major and semi-minor axes of, say, a and b, and the major axes are oriented in the streamwise direction. For steady vortices with spacing l (measured by distance between vortex centres), the thickness of the shear layer is limited by the inequality $2b < 0{\cdot}36\,l$; from this property, the authors conclude that when turbulent diffusion causes the thickness to exceed the bound for steady vortices, the vortices must break up and reorganize into a shear layer with larger l. This process, referred to as 'tearing', is distinct from the conventional pairing process. The thickness bound is derived from the inequality $(ab)^{\frac{1}{2}} < 0{\cdot}3\,l$, so that the tearing criterion can also be expressed as a bound on the area of steady vortices for fixed spacing. While these results are suggestive, they are inconsistent with the assumptions made in deriving the steady states, as the area maximum occurs only when $2a > l$, implying that neighbouring vortices overlap. In the present work, we make use of numerical techniques developed in Pierrehumbert (1980*a*) to relax the assumption of uniform plane strain, replacing it with the actual influence of an infinite row of identically shaped vortices. In this more precise calculation, the area maximum occurs before the neighbouring vortices touch. This result supports the key principle behind the tearing mechanism.

In addition to computing the family of vortex boundaries, we have computed the kinetic energy associated with each member of the family. In §3, it will be seen that energetic constraints place a lower bound on the size of vortex cores resulting from the roll-up of a vortex sheet into a row of vortices of fixed spacing; this argument is similar to that used by Spreiter & Sacks (1951) to predict the structure of aircraft trailing vortices. The energy computation is also used to investigate general features of vortex amalgamation events, including entrainment, core size transitions, and evolution toward self-similarity.

2. Steady-state shear-layer vortices

In two dimensions, the steady Euler equations become simply

$$(\partial_{xx}+\partial_{yy})\Psi = \omega(\Psi), \tag{1}$$

where Ψ is the Stokes stream function and $\omega(\Psi)$ is an arbitrary function. For any choice of the arbitrary function and specification of boundary conditions, (1) defines a nonlinear elliptical problem for Ψ. We will now specialize this problem to the case of the free shear layer. Let x be the mean streamwise direction and y be the direction of the mean velocity gradient. Then, we require that $\Psi \rightarrow +U_\infty y + \text{const.}$ at $y = +\infty$ and $\Psi \rightarrow -U_\infty y + \text{const.}$ at $y = -\infty$. Further, to allow for a coherent vortex structure, we require that Ψ be periodic of period l in the x direction. In most experimental arrangements, this condition will not be met, as the shear layer is generally allowed to develop downstream of a splitter plate or backwards step; the arrangement we have assumed corresponds more nearly to a stage in the development of an infinite parallel shear layer that has been created at an initial instant of time. However, the problem as stated is the more tractable one, and should fairly well reproduce the experimental results so long as we are interested in a stretch of the shear layer containing no more than two or three vortices. There is still considerable freedom in the choice of the arbitrary function. It will be sufficient to consider the function in one cell, say from $x = -\frac{1}{2}l$ to $x = \frac{1}{2}l$, since the stream function and all flow properties are identical from cell to cell. Within the cell, we assume that $\omega = \omega_0$ within some simply connected compact region S bounded by a curve ∂S, and that $\omega = 0$ outside S. With this choice of vorticity distribution, the flow is completely specified by the knowledge of ∂S, and (1) becomes identical to the requirement that ∂S be a streamline, since vorticity is constant within S. This is also the distribution used by Moore & Saffman, and hence most suitable for comparison with their results. Many other choices of f are possible. Stuart (1967), for instance, studied solutions with $f(\psi) = \exp(-\psi)$. The most physically appropriate choice of f depends in a manner not yet understood on the details of the roll-up process which gives rise to the vortices. The comparison between Stuart vortices and uniform vortices as a model of the observed vortices will be discussed later in this section.

Deem & Zabusky (1978) have examined steady and unsteady states of uniform vortices, but have not considered the shear layer configuration. Elsewhere (Pierrehumbert 1980*a*), we considered the structure of a translating pair of contra-rotating vortices, and developed a simple, efficient iterative method for computing the steady boundary shapes. This method can be easily extended to the geometry of interest in the present work. First, we formally invert (1) using the Green's function for the periodic geometry. For uniform vortices this yields

$$\Psi(x,y) = \omega_0 \int\int_S G(x-x', y-y')\, dx'\, dy'. \tag{2}$$

The appropriate Green's function may be found in Lamb (1932), and is given by

$$G(x,y) = (4\pi)^{-1} \ln(\cosh^2(2y) - \cos^2(2x)). \tag{3}$$

Implicit in this choice is the specification that the vortex spacing $l = \pi$. Results for other values of the vortex spacing can easily be obtained by dimensional analysis. By differentiating (2), we easily find that

$$(\hat{x}\partial_x + \hat{y}\partial_y)\Psi = -\omega_0 \int_{\partial S} G(x-x', y-y')(\hat{x}\, dy' - \hat{y}\, dx'), \tag{4}$$

where the path integral is taken in the clockwise sense. We want to find a shape S such that Ψ is constant on ∂S. To this end, we introduce the function $\Delta\Psi = \Psi - \Psi_0$, where Ψ_0 is the value of the stream function at some arbitrary point on ∂S. $\Delta\Psi$ is found by numerically integrating (4) along ∂S. We now assume that S is symmetric about some horizontal line, which we will take as the x axis, and some vertical line, which we will take as the y axis. This assumption is not crucial, but it is a logical simplification, as the vortices will then reflect the symmetry inherent in the problem. The question of whether non-trivial asymmetric solutions exist is beyond the scope of the present work. If we stipulate further that S be convex, ∂S can be completely characterized by its height above the x axis in the $(+,+)$ quadrant, a function we will call $g(x)$. At fixed l, the family of curves satisfying $\Delta\Psi = 0$ can be parametrized by the value of x, say a, at which the curve crosses the positive x axis. Thus, we want to

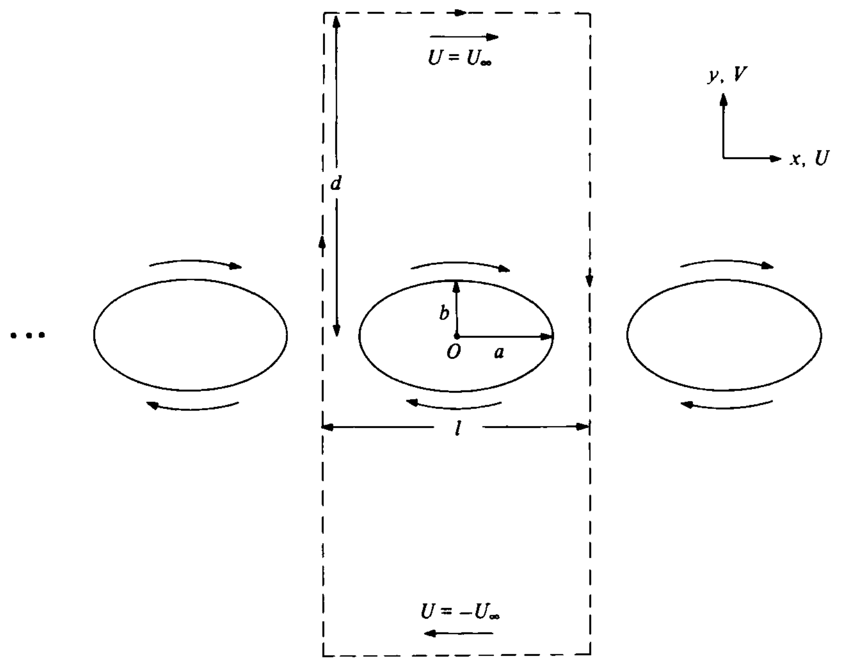

FIGURE 1. A schematic representation of a row of vortices in the form of a shear layer, with defining characteristics. Each curve represents a boundary enclosing a region of constant vorticity, embedded in irrotational fluid, and the row repeats indefinitely to the left and right. The point marked O is the origin of the x, y co-ordinate system used in the analysis.

hold $g(a) = 0$ while varying the function g to obtain $\Delta\Psi = 0$ all along the curve. We may discretize the problem by representing g by its value at a discrete set of points x_j for $j = 1, \ldots, M$. Our previous work showed that the iteration

$$g^{N+1}(x_j) = g^N(x_j) - k\frac{\Delta\Psi(x_j, g(x_j))}{\partial_y \Psi(x_j, g(x_j))} \tag{5}$$

would converge rapidly to a boundary shape that is also a streamline. This is the algorithm we used to calculate g in the present work. g^N is the Nth approximation to the boundary shape and k is an under-relaxation factor. $\Delta\Psi$ is computed relative to $\Psi(a, 0)$ and both $\Delta\Psi$ and Ψ_y in (5) are computed using g^N in (4). Each complete iteration can be performed in $O(M^2)$ operations because (4) is a one-dimensional integral; the iteration process is therefore economical.

The arrangement of vortices we have been considering, along with some defining parameters, is summarized in figure 1. A non-dimensional parametrization of the family of vortices is $W = 2a/l$. Other important non-dimensional vortex characteristics are the aspect ratio $e = b/a$, the shear-layer thickness $H = 2b/l$, and the equivalent vortex radius $R = 2l^{-1}(A/\pi)^{\frac{1}{2}}$, where A is the area of the vortex. For fixed l, R is a monotonic function of the vortex area. Using the procedure described above, we calculated the curve $g(x)$ for a number of values of W up to $W = 0{\cdot}995$. The calculations were done with $M = 50$. Some representative members of this family of curves are shown in figure 2(a). A steady state vortex could always be found, even when the vortices are almost touching. The continuation of the family past the point at which

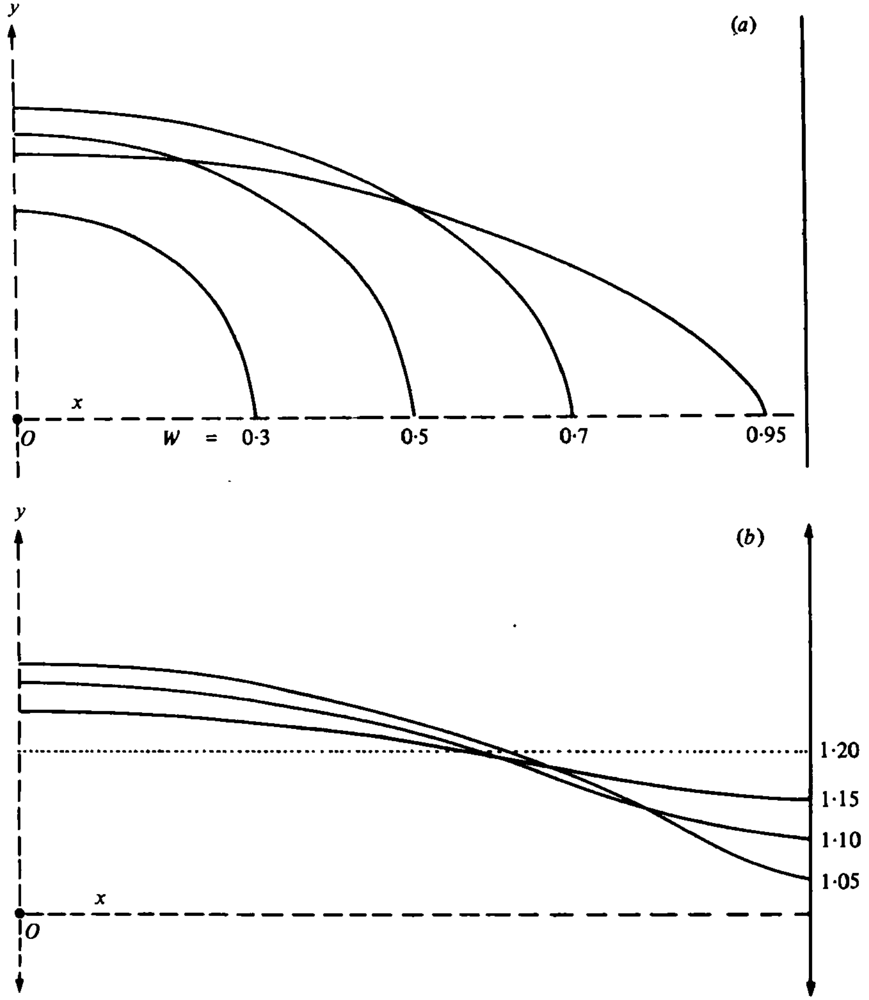

FIGURE 2. (*a*) Representative members of the family of curves $g(x)$ defining possible stationary vortices in a periodic shear layer. Each curve is the boundary in the $(+, +)$ quadrant of a region of constant vorticity embedded in irrotational fluid. Each vortex is symmetric about the two dashed lines giving the x and y axes. The vortices are arranged in a row, as depicted in figure 1, and the vertical solid line is the line of symmetry between the depicted vortices and their neighbours to the right. The numbers on the curves give the value of W (ratio of vortex width to spacing) for the members of the family. (*b*) The same as figure 2(*a*), but for merged vortices. W in this case is $1+2g_1/l$, where g_1 is the minimum height of the curve above the x axis and l is the vortex spacing. The dotted line represents the boundary of the parallel uniform shear layer from which the family bifurcates.

the vortices touch will be discussed shortly. First, we note that the vortices are nearly circular for small W, but become progressively flatter as W is increased. This tendency is also evident in figure 3, where we have plotted the non-dimensional vortex shape characteristics as a function of W. H reaches a maximum of 0·4 at $W = 0{\cdot}7$, as opposed to a maximum of 0·33 for the elliptical vortices treated by Moore & Saffman. The vortex area (measured by R) reaches a maximum at $W = 0{\cdot}87$ for the vortices we have calculated. The existence of an upper bound for the vortex area confirms the basis of the tearing mechanism for shear growth. If a vortex is initially characterized by a value of $W < 0{\cdot}87$, turbulent entrainment of irrotational fluid will cause it to evolve in the direction of increasing area (to the right in figure 3) until the area maximum is reached at $W = 0{\cdot}87$. At this point there is no longer a nearby steady state with greater area into which the vortex can evolve, unless the vortex spacing is allowed to increase. Presumably, then, the vortex breaks up and becomes amalgamated with one or both of its neighbours. This process increases l and allows the vortex to continue evolving in the direction of increasing area. Implicit in this picture is the assumption that no other process (such as subharmonic instability) disrupts the shear layer in the time it takes for entrainment to cause the area maximum to be attained.

The vortex boundary is a well-behaved curve even when neighbouring vortices almost touch. This suggests the existence of solutions in which neighbouring vortices are joined to one another. For such solutions, the vortex boundaries are no longer closed curves; instead, the upper boundary of the region containing vorticity is a continuous periodic curve, and the lower boundary is the reflexion of this curve about the x axis. Using a minor modification of the procedure described above for discrete vortices, it was possible to compute a family of merged vortex solutions. In the modified algorithm, $g_1 = g(\frac{1}{2}l)$ was held fixed as the iteration was performed. The parametrization of the discrete vortices was continuously extended to the family of merged vortices by defining $W = 2g_1/l + 1$ for the merged vortices. In addition to any curved solution $g(x)$, the parallel shear layer with $g(x) \equiv g_1$ is always a solution to the problem as stated; the algorithm always converges to the solution nearest the initial guess, so that the parallel flow solution can be suppressed by a suitable choice of starting values for the iteration, providing an alternate solution exists. Some representative boundary curves for merged vortices are shown in figure 2(*b*). The vortex shape for $W = 1{\cdot}05$ is similar to the shape of elongated discrete vortices, indicating that the family of discrete vortices extends continuously into the family of merged vortices. As W approaches $1{\cdot}2$, the curves become progressively straighter, and at $W = 1{\cdot}2$ only a parallel solution could be found. Hence, the complete family of steady shear layers we have exhibited – merged and discrete – can be viewed as bifurcating from a parallel shear layer with non-dimensional thickness $H = 0{\cdot}2$. Rayleigh (1878) computed the dispersion relation for waves on a parallel shear layer of finite thickness and constant vorticity, and so inadvertently solved this linear bifurcation problem. The dispersion relation predicts vanishing phase velocity (a steady disturbance) when $kh = 1{\cdot}278$, where k is the streamwise wavenumber of the disturbance and h is the dimensional thickness of the layer. Recalling that $H = h/l$ and $k = 2\pi/l$, we find that steady disturbances of infinitesimal amplitude and period l can exist only on a parallel shear layer with $H = 0{\cdot}20$, which is precisely in agreement with our computations. In addition, it is easily verified from results presented by Rayleigh that the steady disturbance represents a displacement of the vortex boundary with the same symmetry as that assumed in our own computations.

The values of R and H for merged vortices may be found in figure 3. Notably, the cross-sectional area for the merged vortices does not exceed the maximum found for discrete vortices, so that our earlier conclusions with regard to the tearing mechanism are unaltered.

The most widely and readily measured characteristic of shear layer vortices is the ratio of maximum-slope thickness of the shear layer (δ_ω) to the vortex spacing (l). This ratio can also be easily calculated for the family of uniform vortices, and is shown

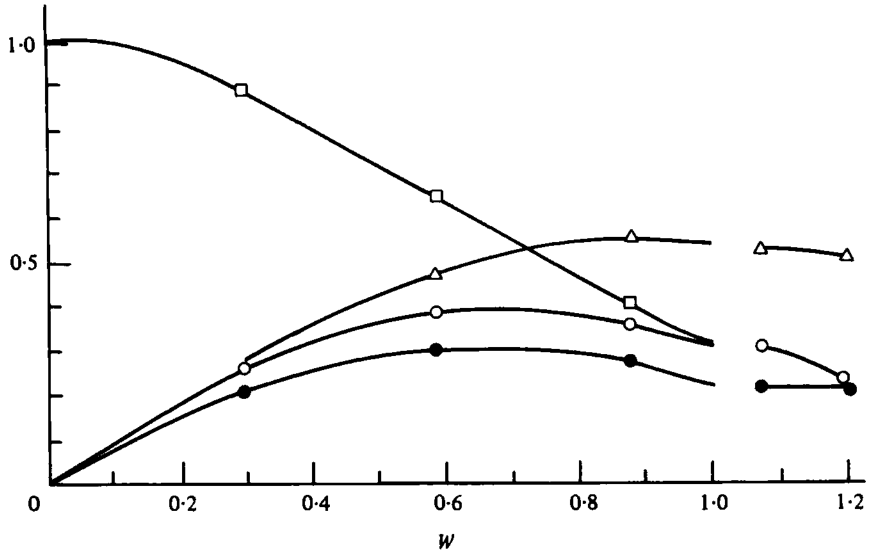

FIGURE 3. Non-dimensional geometric characteristics of the family of vortices, as a function of width parameter W. Values of W greater than unity denote merged vortices. □, aspect ratio $e = a/b$; △, area function $R = 2(A/\pi)^{\frac{1}{2}}/l$; ○, thickness ratio $H = 2b/l$; ●, non-dimensional vorticity thickness δ_ω/l, where δ_ω is the maximum slope thickness of the vortical shear layer.

in figure 3. Brown & Roshko (1974) report average values of $\delta_\omega/l = 0{\cdot}29$ for high-Reynolds-number uniform-density mixing layers with $r = 2(U_1 - U_2)/(U_1 + U_2) = 0{\cdot}36$. Winant & Browand (1974) report average values of 0·30 at the same value of r. Browand & Weidman (1976), working at Reynolds numbers several order of magnitude lower than Brown & Roshko, and at $r = 0{\cdot}85$, report values in the range 0·33 to 0·29, with an average of 0·31.

For the computed vortices, on the other hand, δ_ω/l reaches a maximum of 0·30 near $W = 7$ and falls to 0·27 at $W = 0{\cdot}87$, where tearing occurs. With the exception of the measurement of Brown & Roshko, the observed average values of the thickness ratio are equal to or slightly above the maximum thickness ratio for the steady vortices. Though this slight mismatch indicates that the assumptions of steadiness and uniform vorticity introduce some inaccuracies, the substantive agreement strongly supports the hypothesis that shear layer vortices in between amalgamation events are in a quasi-steady state which can be modelled as a steady state of the Euler equations. We note that Koochesfahani *et al.* (1979) have reported values of δ_ω/l in the range 0·26 to 0·27, which are significantly lower than those previously reported. This is unlikely to be a Reynolds-number effect, as the Reynolds number is intermediate between that investigated by Browand & Weidman and that investigated by Brown & Roshko; nor is it likely to be a result of differing velocity ratio, as the value $r = 0{\cdot}65$ is also within the range of previous investigations. However, instead of measuring δ_ω directly, Koochesfahani *et al.* infer it from measurements of the outer potential flow, assuming that the perturbations to the potential flow field due to the passage of a vortex are the same as would be produced by the passage of an isolated point vortex. The inaccuracies introduced by the latter assumption may account for the difference with earlier observations.

Stuart (1967) discovered that the stream function

$$\Psi = \frac{l\Delta U}{4\pi} \ln\left(\cosh\left(2\pi y/l\right) - \rho \cos\left(2\pi x/l\right)\right)$$

is an exact solution to the two-dimensional Euler equations. ρ is a variable in the range [0, 1] which parametrizes the family; $\rho = 0$ corresponds to a parallel hyperbolic tangent shear profile, and $\rho = 1$ corresponds to a row of singular point vortices. Unlike the uniform vortices, the Stuart vortices for $\rho < 1$ have continuous vorticity distributions. Like the uniform vortices, the Stuart vortices represent a family of solutions that bifurcates from a parallel shear layer and extends continuously to a row of point vortices. The value of δ_ω/l for the Stuart vortices can be computed from (7.12) in Stuart (1967). Unlike the uniform vortices, δ_ω/l for the Stuart vortices decreases monotonically from a maximum value of $1/\pi$ ($\approx 0{\cdot}32$) at $\rho = 0$. This maximum value is slightly larger than that for the uniform vortices, and is more nearly consistent with the range of observed thickness ratios cited above. Using conditional sampling techniques, Browand & Weidman (1976) directly observed the vorticity distribution of an ensemble of typical vortices, and found that the Stuart vortex with $\rho = 0{\cdot}25$ corresponds reasonably well to the observed distribution, save that the observed vorticity drops rather more precipitously at the vortex edge than that for the Stuart vortex. This suggests that a pattern intermediate between that of the uniform vortices and that of Stuart vortices may be most appropriate for the physical situation. It is significant, though, that estimates of maximum thickness ratio differ by under 7 % between the Stuart vortex model and the uniform vortex model.

The observed thickness ratios are all characteristic of rather large vortices, with $W \approx 0{\cdot}7$, rather than pointlike vortices with small W. It is thus natural to inquire as to whether there is some physical principal which prevents the small vortices from being realized. In § 3 we will see that the energetic properties of the steady states provide such an explanation.

3. The energetics of roll-up, pairing and tearing

In this section, we will calculate the energy associated with the family of vortices described in the previous section. Specifically, for each member of the family, we compute the kinetic energy per unit spanwise length in a rectangular region of width l and height d enclosing a single vortex, as represented by dashed lines in figure 1. The height d is chosen to be large enough for the velocity on the horizontal branches of the contour to be essentially horizontal and of uniform magnitude U_∞. Denoting this region by V, the energy is given by

$$T = \tfrac{1}{2}\rho \int_V \int \nabla\Psi \,.\, \nabla\Psi \, dx\, dy. \tag{6}$$

This integral can be simplified using the asymptotic form of Ψ and repeated applications of the divergence theorem. We obtain

$$\frac{T}{\rho} = (2ld)\left(\tfrac{1}{2}U_\infty^2\right) + \frac{\pi^2 U_\infty^2 l^2}{4} T^*, \tag{7}$$

where the dimensionless quantity, T^*, is given by

$$T^* = -\frac{8}{\pi^2\omega_0 A}\Psi_1 + \frac{4}{\pi^2\omega_0 A^2}\int_{\partial S} f\hat{n}.\nabla\Psi\, ds - \frac{4}{\pi^2 A^2}\int_S\int f\, dA - \frac{4}{\pi^3}\ln(2) \tag{8a}$$

with

$$f = \tfrac{1}{2}(x^2+y^2) \tag{8b}$$

for unmerged vortices, and

$$f = y^2 \tag{8c}$$

for merged vortices. The value of Ψ on the vortex boundary, Ψ_1, can be obtained as a one-dimensional integral by applying the divergence theorem to (2) twice and can be evaluated at any point on the boundary. We choose the point $x = 0, y = g(0)$ and find

$$\Psi_1 = \omega_0 \int_{\partial S} \mathbf{r}'.\hat{\mathbf{n}}'\, G(-x'(s), g(0)-y'(s))\, ds - \tfrac{1}{2}\lim_{y\to g(0)_+} \omega_0 \int_{\partial S} f\hat{\mathbf{n}}.\nabla' G(-x', y-y')\, ds \tag{9a}$$

with f defined as before, and

$$\mathbf{r}' = \tfrac{1}{2}(x'\hat{\mathbf{x}} + y'\hat{\mathbf{y}}) \tag{9b}$$

for unmerged vortices and

$$\mathbf{r}' = y'\hat{\mathbf{y}} \tag{9c}$$

for merged vortices. In the case of merged vortices, the integral along the curve ∂S is to be understood as excluding the vertical segments of the boundary where the vortices touch. With these formulae, T^* can be evaluated using one-dimensional integrals alone. The integrands in (9a) both contain singularities, the first being of logarithmic type and the second being of delta-function type. Save for the necessity of handling these singular portions analytically, the evaluation of T^* presents no particular difficulties. Because of non-dimensionalization, T^* is a function of the width parameter W alone.

In order to interpret the results of the energy calculation, it is necessary to prove a simple energy-conservation lemma for unsteady flows. Consider the evolution of a two-dimensional flow with velocity field $\mathbf{q}(x,y)$, periodic in x with period L. The evolution of the kinetic energy density is determined by

$$\partial_t(\tfrac{1}{2}\rho q^2) + \mathbf{q}.\nabla(\tfrac{1}{2}\rho q^2) + \nabla.(\mathbf{q}p) = \upsilon\mathbf{q}.\nabla^2\mathbf{q}, \tag{10}$$

where υ is the viscosity of the fluid. Let V' be a region similar to V as described above, but of width L, and T' be the energy in this region. Then, by integrating (10) over V', we obtain

$$\frac{d}{dt}T' + \int_{-d}^{d} dy[u(\tfrac{1}{2}q^2+p)|_{x=-\frac{1}{2}L}^{\frac{1}{2}}] + \int_{-\frac{1}{2}L}^{\frac{1}{2}L} dx[v(\tfrac{1}{2}q^2+p)|_{y=-d}^{d}]$$
$$= \upsilon\int_{-d}^{d} dy[\mathbf{q}.\partial_x\mathbf{q}|_{x=-\frac{1}{2}L}^{\frac{1}{2}L}] + \upsilon\int_{-\frac{1}{2}L}^{\frac{1}{2}L} dx[\mathbf{q}.\partial_y\mathbf{q}|_d + \mathbf{q}.\partial_y\mathbf{q}|_{-d}] - \upsilon\int_{V'}\int(\nabla\mathbf{q}).(\nabla\mathbf{q})\, dA. \tag{11}$$

The second integrals on the left- and right-hand sides vanish because of the periodicity assumption, whereas the first integrals on the right- and left-hand sides vanish because d has been taken large enough that $\mathbf{q}$ is essentially constant and horizontal on the horizontal portions of the contour $\partial V'$. The remaining term on the right-hand side is strictly negative, and vanishes only if viscosity is neglected. We are left with the result

$$\frac{dT'}{dt} \leqslant 0. \tag{12}$$

This result would remain valid if an eddy diffusion term of the form $(\nabla . \nu(\mathbf{q})\nabla)\,\mathbf{q}$ were used instead of the molecular diffusion term in (10) so long as ν remains positive.

Now consider the transition from an initial steady state to a final steady state, via some intermediate process with (arbitrary, large) period L. Equation (12) then implies that the energy in V' for the final state is not greater than that for the initial state. Suppose the initial and final states have period l_1 and l_2, respectively, so $n_1 l_1 = n_2 l_2 = L$. If the final state is composed of vortices with non-dimensional width W_2, the final state energy is, referring to (7),

$$\frac{T'_f}{\rho} = (2dL)(\tfrac{1}{2}U_\infty^2) + n_2 \frac{\pi^2 U_\infty^2 l_2^2}{4} T^*(W_2). \tag{13}$$

The first term is clearly the energy in V' of a vortex sheet with velocity jump $2U_\infty$; hence, if the initial state is a vortex sheet, (13) and (12) imply

$$T^*(W_2) \leqslant 0. \tag{14a}$$

If the initial state consists of n_1 vortices of width W_1, we have instead

$$n_2 l_2^2 T^*(W_2) \leqslant n_1 l_1^2 T^*(W_1). \tag{14b}$$

When $l_1 = l_2$, so $n_1 = n_2$, we obtain the result that, for fixed spacing, T^* can never increase in a spontaneous process.

Thus, the energetic properties of the family of vortices are characterized by $T^*(W)$. This function, calculated with $M = 100$, is plotted in figure 4.

We are now in position to consider energetic constraints on roll-up, pairing, and tearing. Equation (14a) states that any row of vortices produced by roll-up of a vortex sheet must have T^* negative or zero. From figure 4, we note the expected result that small vortices have large, positive T^*, and so cannot be produced by roll-up. From the point at which T^* becomes negative, we conclude that $W \geqslant 0{\cdot}48$ for vortices produced in this manner. This is fully consistent with the observations cited in §2, though the observed vortices tend to be on the large side, indicating that energy is dissipated in the roll-up process. We refer the reader back to figure 2(a) for an indication of what the minimum width vortex looks like.

An important feature of the curve in figure 4 is that T^* has a minimum, which occurs at a point where the vortex area is at a maximum. This means that when turbulent diffusion has caused W to reach $0{\cdot}87$, there is no longer any steady-state vortex with lower T^* as long as the spacing remains constant; hence, it is likely that at this point the spacing will change, i.e. that the vortex will disperse and join one or both of its neighbours. The tearing mechanism can thus be predicted on the basis of energy considerations as well as on the basis of vortex area. Since the energy curve has a distinct minimum, tearing will occur preferentially at $W = 0{\cdot}87$.

Now suppose pairing occurs, so that two vortices of width ratio W_1 each amalgamate

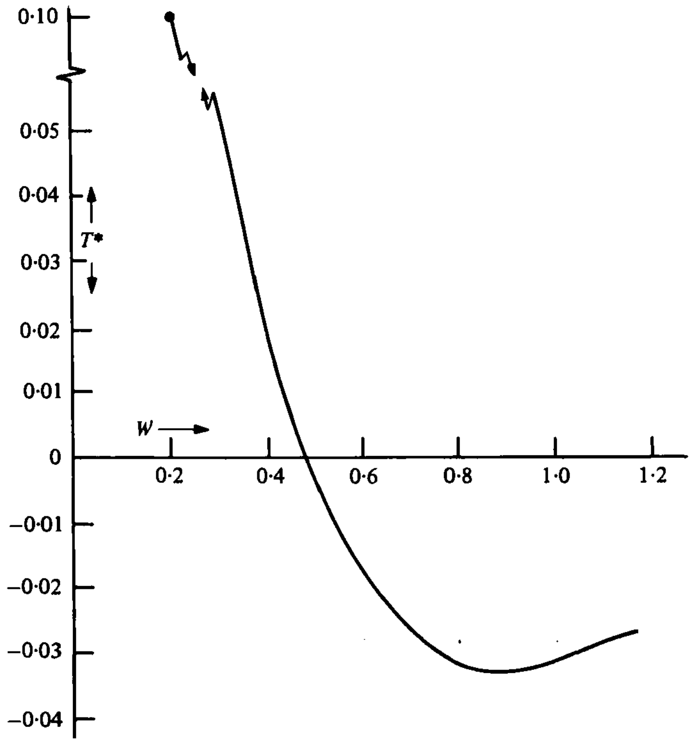

FIGURE 4. The energy curve for the family of shear-layer vortices. T^* is essentially the non-dimensional energy in a length l of the shear layer, in excess of that for a straight vortex sheet. See text for details.

to form a single vortex of width ratio W_2 in the same space. Then, from (14*b*), we infer

$$T^*(W_2) \leqslant \tfrac{1}{2}T^*(W_1). \tag{15}$$

Since T^* is a monotonic decreasing function of W in the region of interest, we conclude that the lower bound on W for a vortex produced by pairing always lies between 0·48 and the value of W for the vortices going into the pairing; the lower bound is attained exactly when the pairing occurs without dissipation of energy. Thus, unless $W_1 = 0{\cdot}48$, the value of W for the shear layer will generally change after pairing, so that pairing does not directly result in self-similar growth of the shear layer. However, from (15), it is evident that each energy conserving pairing halves the magnitude of T^*, so that after not too many conservative pairings $T^* \rightarrow 0$ and $W \rightarrow 0{\cdot}5$, whereafter pairing produces self-similar shear layer growth. This mechanism for evolution toward self-similarity cannot operate unless the dissipation during and between pairings is sufficiently small. In general, we can only say that pairing tends to reduce the vortex width relative to the spacing.

To see that entrainment must occur, we note that the difference in area between the initial two vortices of spacing l and the single vortex they amalgamate into is

$$\Delta A = \pi l^2(R^2(W_2) - \tfrac{1}{2}R^2(W_1)) \tag{16}$$

In the extreme case, $W_1 = 0{\cdot}87$ (so that the initial area is a maximum), (15) and the energy curve in figure 4 predict $W_2 \geqslant 0{\cdot}6$; then $R^2(W_2) - \tfrac{1}{2}R^2(W_1) \geqslant 0{\cdot}07$. Thus, vortex pairing is always accompanied by net entrainment of irrotational fluid. The lower bound is attained for conservative pairing, and any energy dissipation will increase the entrainment. It is also evident from (16) that any self-similar pairing, conservative or otherwise, results in entrainment, since $W_1 = W_2$ for the self-similar case. Moore & Saffman (1975) have pointed out that there is no apparent mechanism which would allow entrainment to occur during pairing but not at other times; hence, it is most likely that turbulent diffusion is continually causing the vortex area to grow and the energy to decrease, until the energy minimum is attained and amalgamation occurs. We have shown that vortex amalgamation tends to decrease the core size relative to spacing, so that after amalgamation the cycle can repeat itself. It may be the average of many amalgamation-diffusion events that is responsible for the observed self-similarity of the free shear layer.

The tearing mechanism could cause three vortices to reorganize into two instead of causing two vortices to reorganize into one. The former sort of vortex transition can be treated using the methods applied to pairing. Suppose three vortices in a length $3l$ reorganize into two in the same length. Then the equivalent of (15) is

$$T^*(W_2) \leqslant \tfrac{2}{3}T^*(W_1). \tag{17}$$

Hence, the conclusions we reached for pairing also apply to this transition, except that in this case tearing tends not to decrease W as much as for pairing; this kind of amalgamation therefore tends to result in a shear-layer growth that is more nearly self-similar, even allowing for turbulent dissipation. The entrained area is now given by

$$A = \tfrac{9}{8}\pi l^2(R^2(W_2) - \tfrac{4}{9}R^2(W_1)) \tag{18}$$

whence it can be found that in this case as well the entrainment never vanishes. The method we have demonstrated can also be applied to vortex tripling, quadrupling, and so forth.

4. Conclusions

We have exhibited a class of steady solutions to the two-dimensional Euler equations which bear a strong resemblance to the coherent vortex structure observed in the free shear layer. For a given vortex spacing, energetic considerations place a lower bound on the width and cross-sectional area of vortices that can be produced by roll-up of a vortex sheet, so that point-like vortices are precluded. Moreover, there is a maximum possible area and minimum possible energy for all steady vortices in a row of fixed spacing. This property forms the basis of the tearing mechanism of shear layer growth, whereby spacing increases via amalgamation events whenever turbulent diffusion of vorticity causes one of the bounds to be violated. Vortex amalgamation – whether by tearing or some other process such as the pairing instability – generally reduces the core size relative to vortex spacing, but never below the minimum value for vortices produced by roll-up. In addition, energetic constraints require that vortex amalgamation always be accompanied by entrainment of irrotational fluid. Self-similar shear-layer growth is seen to be a result not of individual amalgamation events, but rather of amalgamation events followed by relaxation to a similar state via the action of turbulent diffusion, in the time it takes for the next amalgamation to take place.

In this paper we have focused attention on the tearing mechanism of shear layer growth, although the conclusions on initial core size and core size transitions are independent of the tearing mechanism. As we have noted earlier, tearing can only be an important mechanism if instabilities of the vortical shear layer do not disrupt the vortices before tearing can take place. We have completed an investigation of the time scale and character of such instabilities in two and three dimensions (Pierrehumbert 1980*b*); the nature of these instabilities, and the role they play in shear-layer transitions, will be the subject of a future paper.

While this manuscript was in revision, it came to our attention that Saffman & Szeto (personal communication, June 1979) had also solved the problem treated in the present work, though by a different numerical method. The conclusions of Saffman & Szeto are essentially identical to ours. In particular, the values of W for the zero-energy vortex (0·48) and for the minimum energy vortex (0·87) agree to two significant figures. We are grateful to Prof. Saffman and Mr Szeto for the opportunity to verify our results against theirs.

This work was supported by the National Science Foundation under contracts 7414978-ENG and 79-16877-CME, and by the Air Force Office of Scientific Research under contract 79-0006. The numerical work was greatly facilitated by the provision of computer time on the Texas Instruments ASC by the Geophysical Fluid Dynamics Laboratory at Princeton, N.J. A preliminary version of this work was presented at the American Institute of Aeronautics and Astronautics 12th Fluid and Plasma Dynamics Conference; the current version appears here by permission of the A.I.A.A.

REFERENCES

Browand, F. K. & Weidman, P. D. 1976 Large scales in the developing mixing layer. *J. Fluid Mech.* **76**, 127–144.

Brown, G. L. & Roshko, A. 1974 On density effects and large structures in turbulent mixing layers. *J. Fluid Mech.* **64**, 775–816.

Deem, G. S. & Zabusky, N. 1978 Stationary 'V-states', interactions, recurrence, and breaking. In *Solitons in Action* (ed. K. Longren & A. Scott), pp. 277–293. Academic.

Koochesfahani, M. M., Catherasoo, C. J., Dimotakis, P. E., Gharib, M. & Lang, D. B. 1979 Two point LDV measurements in a plane mixing layer. *A.I.A.A. J.* **17**, 1347–1351.

Lamb, O. O. 1932 *Hydrodynamics*, 6th edn, pp. 224–229. Cambridge University Press.

Moore, D. W. & Saffman, P. G. 1971 Structure of a line vortex in an imposed strain. In *Aircraft Wake Turbulence* (ed. J. H. Olsen, A. Goldburg & M. Rogers), pp. 339–353. Plenum.

Moore, D. W. & Saffman, P. G. 1975 The density of organized vortices in a turbulent mixing layer. *J. Fluid Mech.* **69**, 465–473.

Pierrehumbert, R. T. 1980*a* A family of steady, translating vortex pairs with distributed vorticity. *J. Fluid Mech.* **99**, 129–144.

Pierrehumbert, R. T. 1980*b* The structure and stability of large vortices in an inviscid flow. Ph.D. thesis, Massachusetts Institute of Technology.

Rayleigh, J. W. S. 1878 *The Theory of Sound*, vol. 2, p. 393 Dover.

Roshko, A. 1976 Structure of turbulent shear flows: a new look. *A.I.A.A. J.* **14**, 1349–1357.

Saffman, P. G. & Baker, G. R. 1979 Vortex interactions. *Ann. Rev. Fluid Mech.* **11**, 95–122.

Spreiter, J. R. & Sacks, A. H. 1951 The rolling up of the trailing vortex sheet and its effect on downwash behind wings. *J. Aero. Sci.* **18**, 21–32.

Stuart, J. T. 1967 On finite amplitude oscillations in laminar mixing layers. *J. Fluid Mech.* **29**, 417–440.

Winant, C. D. & Browand, F. K. 1974 Vortex pairing: the mechanism of turbulent mixing layer growth at moderate Reynolds number. *J. Fluid Mech.* **63**, 237–255.